J Appl Electrochem (2009) 39:1849–1856
DOI 10.1007/s10800-009-9888-0

ORIGINAL PAPER

Study of the effect of mannitol on ZnNi alloy electrodeposition from acid baths and on the morphology, composition, and structure of the deposit

E. M. de Oliveira · I. A. Carlos

Received: 24 October 2008 / Accepted: 29 March 2009 / Published online: 30 April 2009

Abstract A boric acid bath for ZnNi alloy electrodeposition was developed with mannitol as additive. The deposition process was investigated by cyclic voltammetry. It was found that the current density decreased, due to adsorption of a boric–mannitol complex and/or changes in the morphology, but the initial deposition potential was not affected. At deposition potentials more negative than −1.20 V, the current efficiency obtained was high (80–85%) in all baths studied. The addition of mannitol to the bath led to the formation of the best ZnNi deposits, composed of coalesced globular grains smaller than ∼1 μm in diameter. Also, all of the ZnNi deposits studied consisted of γ, γ_1, and Pt_3Zn phases. The Ni content in the ZnNi deposits produced in the presence of mannitol increased from 6 to 10 wt% only in the range −1.26 to −1.40 V. It is suggested that the ZnNi deposits produced in these baths probably offer sacrificial protection to the substrate.

Keywords Electrodeposited ZnNi alloys · Mannitol–boric complex · Additive · Voltammetry · Boric acid

1 Introduction

ZnNi alloys have been developed with the aim of improving the corrosion resistance of Zn metal deposited on steel, since the Zn deposit has the disadvantage of rapid dissolution [1, 2]. Among the various Zn alloys, ZnNi shows the best corrosion resistance [3]; it is a good inhibitor of hydrogen permeation on metallic substrate [4, 5] and adheres well to the substrate [6]. The ZnNi alloy has also replaced highly toxic Cd deposits [7, 8]. Thus, ZnNi alloys are widely employed in the automotive and aerospace industries [1]. When they are used for catalytic purposes, they are required to have a large active surface with a high Ni content. After caustic leaching, the alloy turns into porous Ni electrodes or Raney Ni. This electrode is used for its small of hydrogen and oxygen evolution overpotential [9, 10].

The ZnNi alloys may provide either sacrificial protection or barrier film protection for steel. In the former, the alloy must have a Ni content below ∼18 wt% [11]. This type of protection is most often used because the alloy acts as a sacrificial film and it may offer protection even when it has defects. It is claimed by some authors that the best sacrificial protection is obtained when the Ni content in the alloy is in the range 10–15 wt% [12], while others prefer the range 15–18 wt% Ni [11].

ZnNi alloys have been deposited from both alkaline and acid plating baths. Acid plating is utilized more often, owing to its high deposition rate and cathodic efficiency. Moreover, this bath does not require Ni complexing agents, leading to a less expensive deposition process than alkaline plating [13].

Plating baths containing ammonium chloride are widely used, although nowadays there is a strong trend towards replacing the ammonium chloride by another electrolyte, owing to the difficulty of removing the nickel from the waste electrolyte, which has limited its use [13]. Thus, boric acid has been used as a substitute for ammonium chloride, and in addition to this, other compounds have also been added to the bath, viz. sorbitol or glycerol, with good results [14]. Research on the influence of the polyalcohols like sorbitol, glycerol, and mannitol on the electrodeposition of other metals or alloys [15–17] has shown excellent

E. M. de Oliveira · I. A. Carlos (✉)
Departamento de Química, Universidade Federal de São Carlos, CP 676, 13565-905 São Carlos, SP, Brazil
e-mail: diac@ufscar.br

results, with the formation of smooth deposits that do not burn, even in the potential region of high hydrogen evolution. Moreover, these organic additives are not toxic.

In this article, the effect of adding mannitol to a ZnNi alloy plating bath containing boric acid is described. The electrodeposition process was studied potentiodynamically and the morphology, composition, and structure of the ZnNi deposits were investigated by scanning electron microscopy (SEM), energy-dispersive X-ray spectroscopy (EDS), and X-ray diffraction spectroscopy (XRD), respectively.

2 Experimental details

All experiments were carried out at room temperature (25°C), in a glass single-compartment cell of 50 mL capacity. A platinum disc (0.16 cm^2), a platinum plate ($\sim$2 cm^2), and a calomel electrode (1 M KCl) were employed as working, auxiliary and reference electrodes, respectively. The platinum-working electrode was chosen instead of, for example, a steel electrode, because in the study of dissolution and current efficiency, the steel electrode could dissolve simultaneously to the Zn–Ni alloy, adding a spurious dissolution current. Moreover, in this research a new plating bath was developed for ZnNi electrodeposition, and thus an inert substrate such as platinum should be used, to study this process with minimal interference. Immediately before each experiment, the Pt working electrode was ground with 0.3 μm alumina, immersed in concentrated sulphuric–nitric acid solution (1:2 v/v) and then rinsed with deionized water. The pH of the freshly prepared plating bath, without mannitol ($C_6H_{14}O_6$), was initially $\sim$4.0. However, it was found that after a few deposition voltammetric cycles, the pH of this bath decreased to $\sim$3.0 and remained approximately constant at this value. Therefore, the pH of the fresh ZnNi bath without mannitol (ZnNi1, Table 1), was adjusted to $\sim$3.0 with H_2SO_4. The fall in the pH from 4.0 to 3.0 was probably due to the oxidation of water at the anode during electrodeposition. The plating baths containing mannitol had an initial pH of 2.80 (0.26 M mannitol), 2.60 (0.39 M mannitol), and 2.50 (0.52 M mannitol). The deposition current efficiency (CE) was calculated from the dissolution/deposition charge ratio. The ZnNi deposits were produced potentiostatically at various deposition potentials (deposition time of 40 s), and dissolved voltammetrically. Deposition and dissolution charges were measured with a digital coulometer, model 179-PAR. Preliminary tests were necessary to choose the best conditions for dissolution of the electrodeposits. These were run in 1 M NH_4Cl solution at various pH (1.0, 1.5, and 2.0) and sweep rates (10, 20, and 30 mV s^{-1}). The best conditions were 1 M NH_4Cl, pH 1.5, and 30 mV s^{-1}. At 1 M NH_4Cl and pH 1.0 (all sweep rates) and at 1 M NH_4Cl and pH 1.5 (sweep rates of 10 mV s^{-1}) chemical dissolution was observed. However, at pH 2.0 (all sweep rates) the electrodeposits did not dissolve completely. The experimental error was 2%.The pH was measured with a Micronal B474 pH meter. Potentiodynamic curves were recorded with a *E.G&G* PAR electrochemical system consisting of a model 173 potentiostat/galvanostat. SEM and EDS measurements were made with a Philips FEG XL 30 electron microscope. XRD patterns of the ZnNi deposit surface were produced with Cu Kα radiation (1.5406 Å), using a Rigaku Rotaflex RU200B goniometer, in 2 θ scanning mode (fixed $\theta = 2^\circ$).

Table 1 Composition of deposition baths of ZnNi alloy

Baths
ZnNi1[a]
ZnNi1 + 0.26 M mannitol
ZnNi1 + 0.39 M mannitol
ZnNi2[b] + 0.52 M mannitol

[a] ZnNi1 = 0.55 M $ZnSO_4$ + 0.22 M $NiSO_4$ + 0.33 M $NiCl_2$ + 0.13 M H_3BO_3

[b] ZnNi2 = 0.55 M $ZnSO_4$ + 0.22 M $NiSO_4$ + 0.33 M $NiCl_2$ + 0.26 M H_3BO_3

3 Results and discussion

3.1 Electrochemical studies of the deposition and dissolution process of the ZnNi alloy

Figure 1 shows voltammetric curves of ZnNi deposition from plating baths with various mannitol concentrations. As can be seen, the deposition current density (j_d) decreased as mannitol was added to the bath. Comparing j_d at the peak potential, $E_p = -1.35$ V, in the absence and presence of 0.52 M mannitol, it can be seen that in the latter case j_d was reduced by $\sim$41%. It has been reported that boric acid and polyalcohols react in the molar ratio 1:2, respectively, to form a boric–polyalcohol complex [18, 19]. In the present case, in the baths containing 0.13 M boric acid and 0.26 M (• • •) or 0.39 M (- - -) mannitol, 0.13 M boric–mannitol complex was formed, while in those containing 0.26 M boric acid and 0.52 M (— • —) mannitol, 0.26 M complex was formed.

The lower values of j_d in baths containing mannitol (Fig. 1) was due to adsorption on the Pt surface, during the deposition process, of the boric–mannitol complex and/or modification of the morphology of the Zn–Ni electrodeposit [15]. Also, the presence of mannitol in the solution hindered the diffusion of Zn^{2+} and Ni^{2+} ions, and consequently the cathodic peak became a cathodic wave. Moreover, this behavior was more marked when the

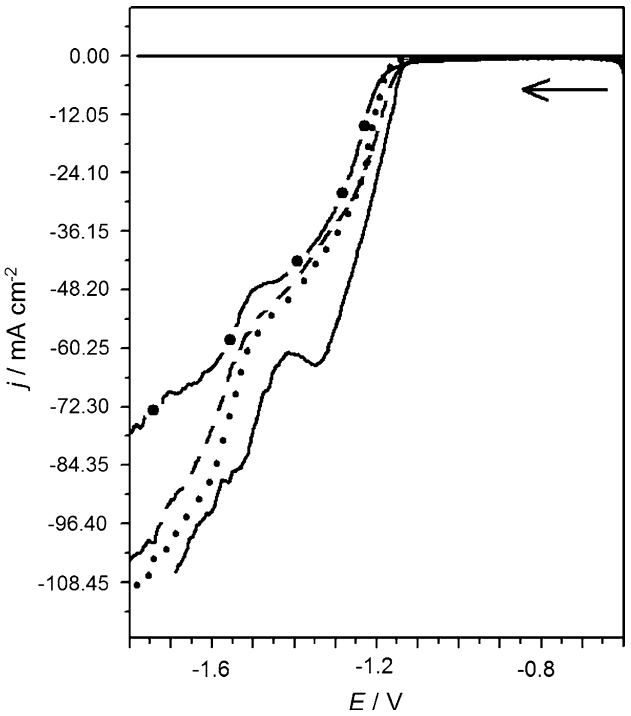

Fig. 1 Voltammetric curves of ZnNi alloy deposition from electrolytic solutions: ZnNi1 (—); ZnNi1 + 0.26 M mannitol (• • •); ZnNi1 + 0.39 M mannitol (– –); and ZnNi2 + 0.52 M mannitol (– • –) (Table 1); $\upsilon = 10$ mV s^{-1}

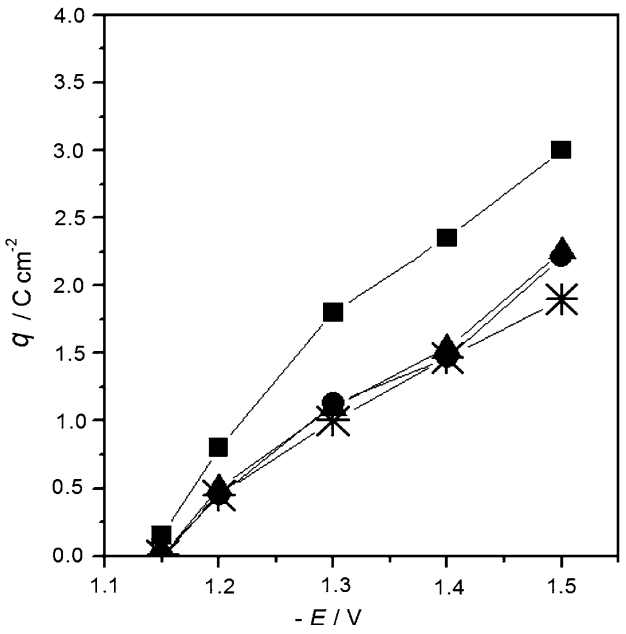

Fig. 2 ZnNi alloy dissolution charge density (q_{diss}) versus deposition potential (E_D). The deposits were produced chronoamperometrically, in a deposition time of 40 s, from the baths: ZnNi1 (*filled square*); ZnNi1 + 0.26 M mannitol (*filled circle*); ZnNi1 + 0.39 M mannitol (*filled triangle*); and ZnNi2 + 0.52 M mannitol (*asterix*) (Table 1)

mannitol concentration increased from 0.26 M (- - -) to 0.52 M (- • -).

It can be observed that in the potential range from −1.20 to −1.40 V, the deposition voltammetric curve was independent of the boric–mannitol complex concentration in the baths. By contrast, for E_d more negative than −1.40 V, the j_d decreases with the addition of 0.52 M mannitol (0.26 M of boric–mannitol complex). Also, Fig. 1 shows that the initial deposition potential ($E_{d,I}$), −1.15 V, did not change in any of the baths studied, implying that no complex was formed between zinc or nickel ions and the boric–mannitol anion. This result corroborates those previously obtained in our laboratory [14–16].

Figure 2 shows the voltammetric dissolution charge density (q_{diss}) of ZnNi deposits produced in baths without and with various amounts of mannitol (Table 1), in the same deposition time (40 s), plotted against deposition potential (E_d). It can be observed that the bath without mannitol (ZnNi1) showed the highest q_{diss} and consequently the highest deposition charge density, while the deposits produced from baths containing various mannitol concentrations all showed the same q_{diss} in the potential range from −1.20 to −1.40 V and, for ZnNi2 + 0.52 M of mannitol alone, a lower q_{diss} at $E_d = -1.50$ V. These results corroborate those in Fig. 1 and indicate that the boric–mannitol complex competes with Zn^{2+} and Ni^{2+} cations for active sites on the Pt substrate.

Figure 3a, b show deposition and dissolution curves obtained from electrolytic solutions ZnNi1 (—) and ZnNi2 + 0.52 M mannitol (— • —), with two different cathodic sweep reversal potentials, −1.26 and −1.55 V. Petrauska et al. [20] report that the boric acid in the plating bath inhibits zinc deposition and favors nickel deposition as the deposition potential becomes more negative. Comparing Fig. 3a and b, it can be seen that there was indeed a rise in the area of anodic peaks a_3 and a_4 (phases rich in nickel) for the bath without mannitol (ZnNi1), when the reversal potential became more negative (from −1.26 V to −1.55 V), corroborating the work of Petrauska et al. For the bath containing mannitol (0.52 M), the dissolution curves show that the ratio of the anodic peak areas $(a_1 + a_2)/(a_3 + a_4)$ was roughly unity, showing that the mannitol did not favor the deposition of either of the metals, zinc or nickel. These results suggest that the ZnNi alloys formed were probably heterogeneous and also that the contents of Zn and Ni in the deposits were different for baths without and with mannitol.

Muller et al. [21, 22] report that their X-ray diffractograms of Zn–Ni electrodeposits always correspond to the γ-phase, and that during dissolution of these deposits, the anodic peaks A and B correspond mainly to the oxidation of zinc from the γ-phase, besides η-phase. Although latter was not detected by XRD analysis, it was formed at a lower concentration. The anodic peak C corresponds to a phase transition → α during the oxidation the -phase Zn [22, 23].

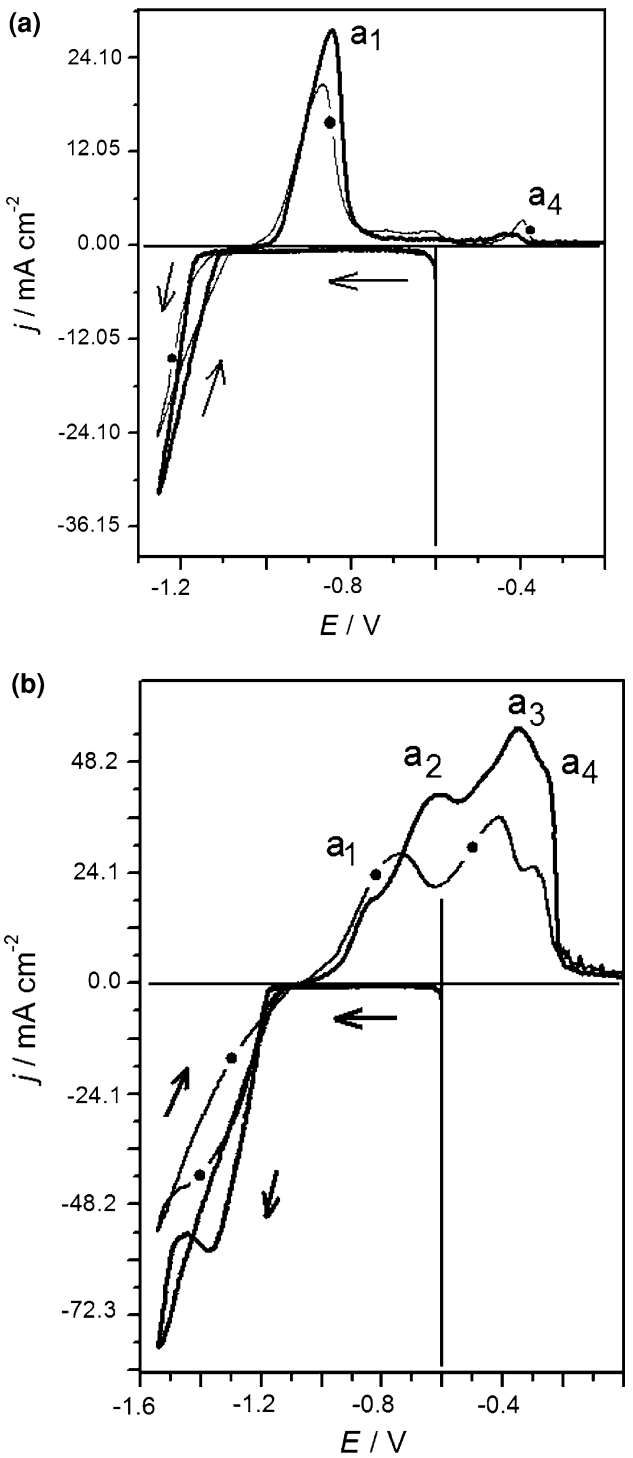

Fig. 3 Voltammetric curves of ZnNi alloy deposition and dissolution from electrolytic solution ZnNi1 (—) and ZnNi2 + 0.52 M mannitol (— • —) (Table 1) with two different cathodic sweep reversal potentials: **a** −1.26 V and **b** −1.55 V; $\upsilon = 10$ mV s^{-1}

Swathirajan [23] also considers the possibility of a transition → β. Lastly, peak D arises from the oxidation of porous Ni [21, 22]. These findings can thus explain all four anodic peaks in Fig. 3b.

The same profile was observed for the deposition process in the baths containing 0.26 and 0.39 M mannitol (Figures not shown).

3.2 Analysis of the ZnNi alloy composition and current efficiency of the cathodic process

EDS analyses of ZnNi deposits laid down chronoamperometrically in baths without and with various mannitol concentrations were carried out, to determine the influence of the polyalcohol concentration and E_d on the percentage of Ni in the ZnNi deposits.

Figure 4a–d show the Ni content (wt%) in the ZnNi deposits for various E_d and bath compositions. In a previous paper [14], it was reported that the ZnNi deposits obtained from solutions without polyalcohol show an increase from ∼6 to ∼20 wt% Ni in the deposits, as E_d becomes more negative, from −1.26 to −1.55 V (Fig. 4a). These results corroborate the voltammetric deposition curves (Fig. 3a, b), as the Ni content in ZnNi deposited from ZnNi solutions with H_3BO_3 increases with increasing polarization.

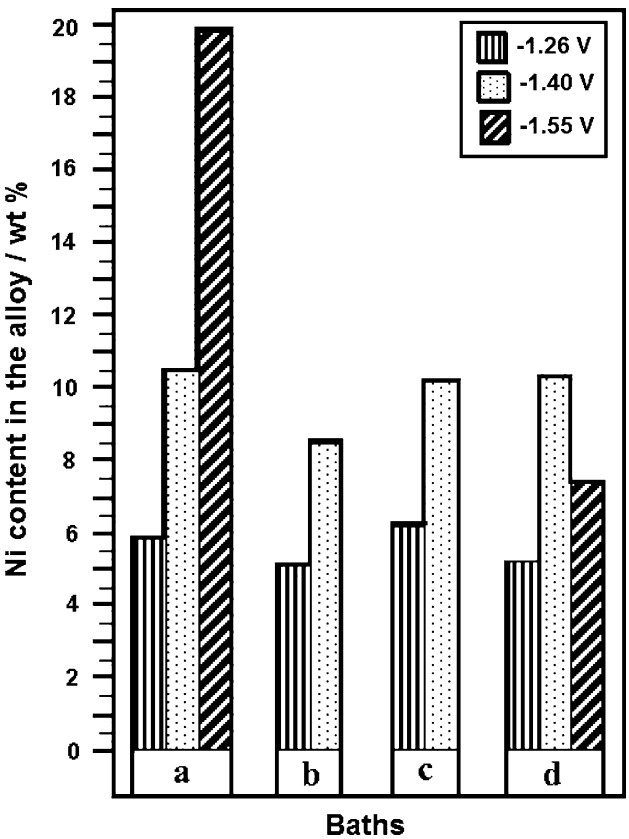

Fig. 4 Ni content (wt%) in the ZnNi alloy produced chronoamperometrically at −0.20 to −1.26 V, −1.40 and −1.55 V (q 4 C cm^{-2}), in baths: **a** ZnNi1, **b** ZnNi1 + 0.26 M mannitol, **c** ZnNi1 + 0.39 M mannitol, and **d** ZnNi2 + 0.52 M mannitol (Table 1)

The relative amount of Ni in the ZnNi deposited from baths containing 0.52 M mannitol remained in the range 5–10 wt% as E_d shifted to more negative potentials, i.e., from −1.26 to −1.40 V (Fig. 4d). In this potential range, the boric–mannitol complex favors Ni deposition, but at E_d more negative than −1.40 V, a small fall in the Ni percentage from 10 to 7.5 wt%, can be observed. Thus, it cannot be concluded that the boric–mannitol complex increased the Ni percentage in the alloy when the E_d became more negative, as observed in the bath without polyalcohol (Fig. 4a).

Figure 4b–d show that there was no significant shift in the Ni content in the deposits as the concentration of mannitol varied, at the same E_d (−1.26 or −1.40 V).

EDS analysis of the ZnNi electrodeposits led to the conclusion that the Zn and Ni codeposition was of the anomalous type.

It has been pointed out [11, 12] that ZnNi deposits containing between 10 and 15 wt% Ni [12] or between 15 and 18 wt% Ni [11] give better sacrificial protection of steel against corrosion than those outside these ranges. Thus, ZnNi deposits providing sacrificial protection can be obtained in baths without mannitol in the region of ∼−1.40 to ∼−1.55 V, and in baths containing mannitol only at the potential ∼−1.40 V (see Fig. 4a–d).

Figure 5 shows the current efficiency (CE) of ZnNi deposition in plating baths without and with various mannitol concentrations. Current efficiency values lower than 100% can be attributed to the hydrogen evolution reaction (HER) taking place simultaneously to the deposition process. Also, at E_d −1.15 V, the CE values were appreciably lower than those attained at more negative E_d. These results imply that in the initial moments of the reduction process ($E_d = -1.15$ V), the HER on Pt substrate is more significant than ZnNi deposition, particularly in the presence of mannitol. For E_d more negative than −1.20 V, the CE values were greater than 80%, both in baths without mannitol and in those with mannitol. The rise in the CE at E_d more negative than −1.20 V was due to an increase in the j_d of Zn and Ni, with formation of Zn–Ni alloys, and consequently a shift in the HER overpotential to more negative potentials. When the E_d became more negative than −1.60 V, the CE fell, mainly in baths without mannitol, and at $E_d = -1.70$ V the fall was 10% relative to baths with mannitol. This fall in the CE was due to the significant HER at this E_d, which led to formation of burned ZnNi deposit (observed by naked eye).

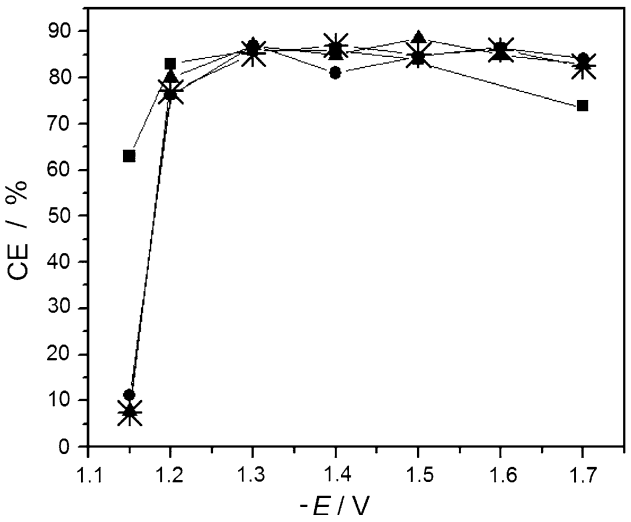

Fig. 5 ZnNi alloy deposition current efficiency (CE) at several deposition potentials and a deposition time of 40 s. Plating baths: ZnNi1 (*filled square*); ZnNi1 + 0.26 M mannitol (*filled circle*); ZnNi1 + 0.39 M mannitol (*filled triangle*); and ZnNi2 + 0.52 M mannitol (asterix) (Table 1)

3.3 Morphological analysis of ZnNi deposits

Figure 6a–d show micrographs of the ZnNi deposits obtained chronoamperometrically from −0.20 to −1.26 V, with a charge density (q) of 4 C cm^{-2}. It can be seen that the ZnNi deposits produced in the presence of mannitol (Fig. 6b–d) were compact, formed of globular grains, the most refined grains being ∼1 μm, while the deposits laid down in the bath without polyalcohol were formed of irregular grains of size ∼2 μm (Fig. 6a).

The ZnNi deposits obtained at $E_d = -1.40$ V in the presence of mannitol (Figure. 7b–d) show a great difference in morphology from that formed in the absence of mannitol (Fig. 7a). In the latter case the deposit was not at all compact, with a grain size of ∼5 μm and consequently it was rough. In contrast, ZnNi deposits produced in baths containing mannitol (Fig. 7b–d) were highly compact, constituted by coalesced globular crystallites, smaller than ∼1 μm. Although no significant difference was observed in the morphology of ZnNi deposits obtained in the presence of mannitol, at −1.40 V or at −1.26 V, the most compact ZnNi deposit was obtained at −1.40 V with 0.52 M mannitol (Fig. 7d).

These results corroborate the voltammetric studies (Fig. 1), which indicated that the adsorption of boric–mannitol complex on the Pt substrate, during the deposition, led to formation of ZnNi deposits with more refined grains and consequently reduction in current density. Thus, the boric–mannitol complex works as a grain refiner and smoother. Also, these results corroborate those for ZnNi electrodeposition in the presence and absence of sorbitol, reported in an earlier study [14].

EDS analysis of ZnNi deposits obtained at −1.40 V without and with mannitol (Fig. 4a–d) and morphological analysis of the deposits (Fig. 7a–d) show that no direct correlation can be made between deposit morphologies and

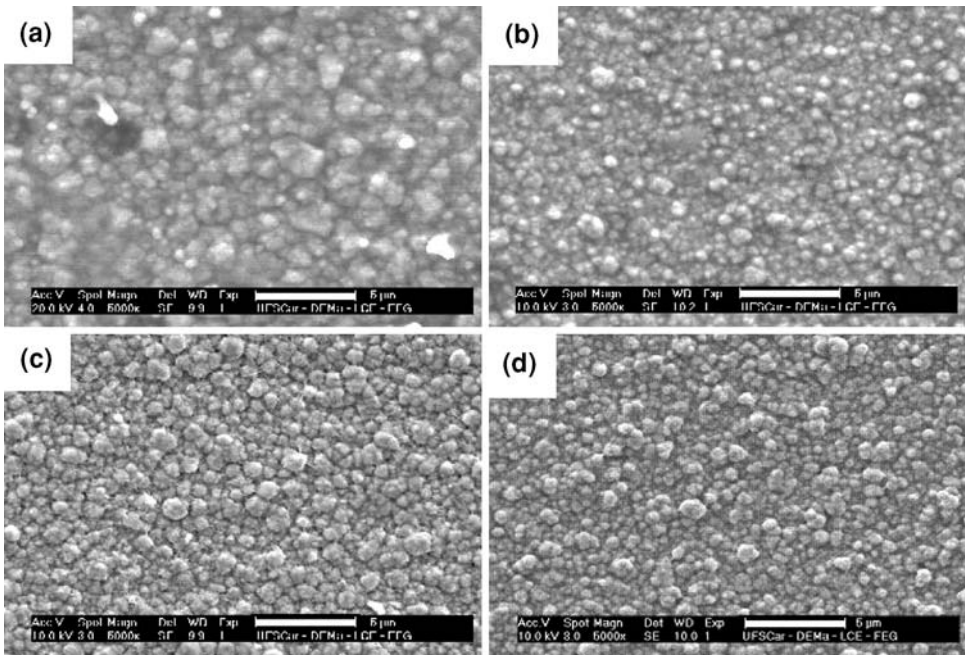

Fig. 6 **a–d** SEM micrographs of ZnNi alloy films obtained chronoamperometrically from −0.20 V to −1.26 V with q 4.0 C cm^{-2}. Electrolytic solutions: **a** ZnNi1; **b** ZnNi1 + 0.26 M mannitol; **c** ZnNi1 + 0.39 M mannitol; and **d** ZnNi2 + 0.52 M mannitol (Table 1); *scale bar* 5 μm

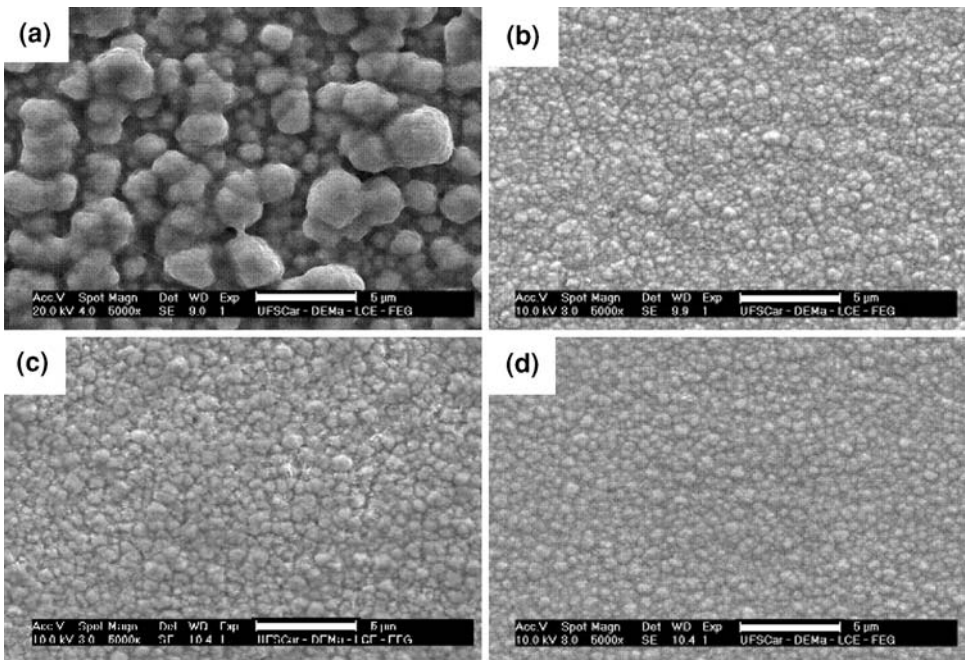

Fig. 7 **a–d** SEM micrographs of ZnNi alloy films obtained chronoamperometrically from −0.20 V to −1.40 V with q 4.0 C cm^{-2}. Electrolytic solutions: **a** ZnNi1; **b** ZnNi1 + 0.26 M mannitol; **c** ZnNi1 + 0.39 M mannitol; and **d** ZnNi2 + 0.52 M mannitol (Table 1); *scale bar* 5 μm)

Ni content. At $E_d = -1.40$ V, the Ni content in the deposits lay between ∼9 and ∼10 wt%, in all ZnNi deposits. However, the ZnNi deposit produced from the bath without mannitol had a morphology completely different from those obtained in baths containing mannitol.

3.4 X-ray analysis of ZnNi deposit

Figures 8a, b and 9a–d show typical X-ray diffraction patterns of ZnNi deposits obtained with q of 4 C cm^{-2} at −1.26 and −1.40 V, respectively, from solutions without (ZnNi1) and with various mannitol concentrations. The X-ray diffractograms indicate that at both potentials there was, in all cases, a mixture of γ (Zn_{21}-Ni_5), γ_1 (Zn_3Ni), and Pt_3Zn phases in the ZnNi deposits. Moreover, the X-ray diffractograms also suggested the occurrence of the δ-phase. Although, the formation of the δ-phase by the electrodeposition process has been reported in the literature [6, 23], its formation is still controversial, as this phase has not been readily obtained by this process [12, 24].

Finally, these results are also consistent with the EDS analysis (Fig. 4), where Zn was present in larger amounts

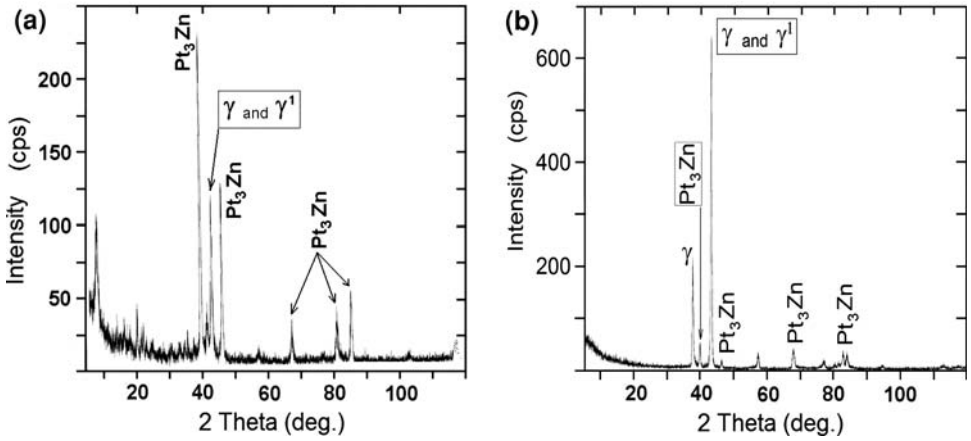

Fig. 8 X-ray diffraction patterns of ZnNi alloy obtained chronoamperometrically from −0.20 V to −1.26 V with q 4.0 C cm^{-2}, from baths: **a** ZnNi1 and **b** ZnNi2 + 0.52 M mannitol (Table 1)

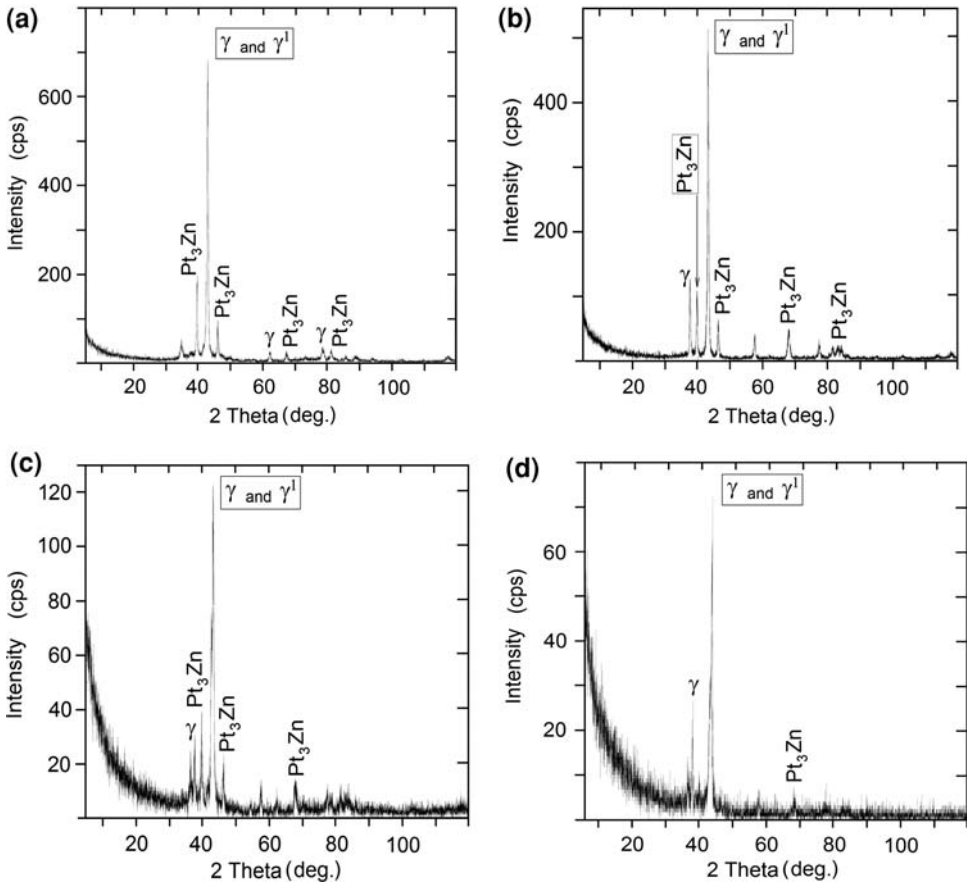

Fig. 9 **a–d** X-ray diffraction patterns of ZnNi alloy obtained chronoamperometrically from −0.20 V to −1.40 V with q 4.0 C cm^{-2}, from baths: **a** ZnNi1; **b** ZnNi1 + 0.26 M mannitol; **c** ZnNi1 + 0.39 M mannitolp; and **d** ZnNi2 + 0.52 M mannitol (Table 1)

than Ni, and also with the ZnNi potentiodynamic deposition studies (Fig. 3a, b), which suggested that ZnNi deposits could be heterogeneous, i.e., a mixture of alloys with high Zn content.

4 Conclusions

ZnNi alloys were successfully deposited from baths containing mannitol. Potentiodynamic studies showed that during deposition there was a decrease in j_d due to the adsorption of the boric–mannitol complex on the Pt substrate and/or a changing deposit morphology and that no complex was formed between Zn^{2+} or Ni^{2+} ions and the boric–mannitol complex. The highest current efficiency values (80–85%) were reached at potentials more negative than −1.20 V, in all baths studied.

SEM examination revealed that among the ZnNi deposits produced at −1.26 or at −1.40 V, in all baths containing mannitol, there was no significant difference in

morphology: all of them consisted of coalesced globular crystallites. The best ZnNi deposits were obtained at E_d −1.40 V, in the presence of mannitol, these being highly compact and constituted by coalesced globular crystallites, smaller than ∼1 μm.

X-ray analysis of the ZnNi deposits produced at −1.26 and at −1.40 V, in all baths, indicated the presence of γ, γ_1, and Pt_3Zn phases.

EDS analysis showed that the Ni content in the ZnNi deposits laid down in the absence of mannitol increased from ∼6 to ∼20 wt% as the E_d changed from −1.26 to −1.55 V. However, in the presence of mannitol, there was a rise in the Ni content from 6 to 10 wt%, only in the range −1.26 to −1.40 V. At E_d more negative than −1.40 V, there was a fall in the Ni percentage. Also, at the same deposition potential, there was no significant difference in the Ni percentages with different mannitol concentrations. It is suggested that the ZnNi deposits generated in these baths can probably offer sacrificial protection to the substrate against corrosion.

Acknowledgments Financial support from the Brazilian agencies CNPq and FAPESP are gratefully acknowledged.

References

1. Pushpavanam M (2000) Bull Electrochem 16:559
2. Kim H, Popov BA, Chen KS (2003) J Electrochem Soc 150:C81
3. Brenner A (1963) Eletrodeposition of alloys, vol 2. Academic Press, New York
4. Coleman DH, Popov BN, White RE (1998) J Appl Electrochem 28:889
5. Ramasubramanian M, Popov BN, White RE (1998) J Electrochem Soc 145:1907
6. Rodriguez-Torres I, Valentin G, Lapicque F (1999) J Appl Electrochem 29:1035
7. Hsu GF (1984) Plat Surf Finsh 71:52
8. Fratesi R, Roventi G (1992) J Appl Electrochem 22:657
9. Karwas C, Hepel T (1989) J Electrochem Soc 138:1672
10. Sheela G, Pushpavanam M, Pushpavanam S (2002) Int J Hydrog Energ 27:627
11. Pushpavanam M, Natarajan SR, Balakrishnan K, Sharma LR (1991) J Appl Electrochem 21:642
12. Hall DE (1983) Plat Surf Finish 70:59
13. Mertens MLAD (2007) Tratam Superf 142:42
14. Oliveira EM, Carlos IA (2009) J Appl Electrochem. doi: 10.1007/s10800-009-9801-x
15. Oliveira EM, Finazzi GA, Carlos IA (2006) Surf Coat Technol 200:5978
16. Oliveira EM, Carlos IA (2008) J Appl Electrochem 38:1203
17. Finazzi GA, Oliveira EM, Carlos IA (2004) Surf Coat Technol 187:377
18. Kolthoff IM, Lingane JJ (1952) Polarography. Interscience, New York
19. Bassett J, Denney RC, Jeffery GH, Mendham J (1978) Vogel's textbook of inorganic quantitative analysis, 4th edn. Longman, New York
20. Petrauskas A, Grincevicience L, Cesuniene A, Matulionis E (2005) Surf Coat Technol 192:299
21. Pushpavanam M, Balakrishnan K (1996) J Appl Electrochem 26:283
22. Elkhatabi F, Sarret M, Muller C (1996) J Electroanal Chem 404:45
23. Swathirajan S (1986) J Electrochem Soc 133:671
24. Cavallotti PL, Nobili L, Vicenzo A (2005) Electrochim Acta 50:4557